Trends in Phytochemical Research (TPR)

Journal Homepage: http://tpr.iau-shahrood.ac.ir

Original Research Article

Molecular simulation of polyketides isolated from the endophyte *Phialophora verrucosa*

Reda Ahmed Abdelhamid[1], Alaa Mohamed Nafady[1], Mohamed Ezzat Abouelela[1], Hiroyuki Konno[2] And Ehab Saad El-khayat[1,*] ✉

[1]Department of Pharmacognosy, Faculty of Pharmacy, Al-Azhar University, Assiut Branch, P.O. Box 71524, Assiut, Egypt
[2]Department of Biochemical Engineering, Graduate School of Science and Engineering, Yamagata University, Yonezawa, Yamagata 992-8510, Japan

ABSTRACT

Endophytic fungi are a wealth of new bioactive metabolites with vast applications in drug discovery. The methyl alcohol extract obtained from the culture of the *Phialophora verrucosa* Medlar., the endophytic fungus of *Senecio flavus* (Asteraceae), was found to be cytotoxic to HepG2 and MCF-7 cell lines (IC_{50} of 20.01 and 28.44 µg/mL), respectively, compared to 5-flurouracil (IC_{50}, 11.05 and 12.46). A chromatographic study led to the isolation of five polyketides; 3,6,7-trihydroxy-α-tetralone **1**, 6-hydroxyisosclerone **2**, 2,3-dihydro-8-hydroxy-2-methyl-benzopyran-1-one **3**, altechromone A **4** and aloesol **5**. Compounds **2**, **4** and **5**, are isolated for the first time from the genus *Phialophora*. Molecular docking analysis simulation was applied to evaluate the inhibitory activities of the isolated compounds against vascular endothelial growth factor receptor (VEGFR2), and cyclin-dependent kinases (CDKs), to illuminate the compounds responsible for the extract cytotoxic activity. Compounds **1** and **5** showed promising results and binding affinities to the examined enzymes.

ARTICLE HISTORY

Received: 07 December 2019
Revised: 07 January 2020
Accepted: 21 January 2020
ePublished: 04 March 2020

KEYWORDS

CDK
Molecular docking
Phialophora verrucosa
Polyketides
VEGFR2

1. Introduction

The inspiring isolation of taxol from *Pestlotiopsis microspora* and its introduction to the drug market, has recognized fungal endophytes as a valuable and attractive approach for new anticancer molecules (El-khayat et al., 2012) as cytochalasins, camptothecin, hypericin, vincristine, and anhydrofusarubin (Zhao et al., 2013; Sharma et al., 2019). Plant endophytes are a source of interesting compounds with an array of biological activities (Strobel and Daisy 2003; Chowdhury et al., 2017), including antioxidant, anticancer, antidiabetic, anti-leishmaniasis, antimicrobial, and antiviral behaviours (Sharma et al., 2019). The current study planned to investigate the cytotoxic fraction of *Phialophora verrucosa*. Several secondary metabolites including azaphilone (Nalli et al., 2015), benzopyrans (Gray et al., 1999), and tetracyclic altenusin (Ye et al., 2013) were isolated from the genus *Phialophora* in addition to polyketides (He et al., 2016). The polyketides are a structurally diverse class of natural products produced by fungi (Weissman and Leadlay, 2005), they have varied biological characteristics as antibiotic, anticancer, antifungal, anti-parasitic, immunosuppressive, and neurotoxic activities (Rocha-Santo and Duarte, 2014).

Molecular docking simulation is a valuable tool for assessing the biological activities of natural products, especially when it comes to solve the issue of amount limitation. It restores the importance of drug discovery and development from natural products as it depends on the prediction of the possible binding modes of

✉ Corresponding authors: Ehab Saad El-Khayat
Tel: 002 088 2080711; Fax: +23422411768
E-mail address: elkhayat@azhar.edu.eg, elkhayatehab@gmail.com

compounds to receptors involved in the biological processes (Meng et al., 2011). Docking used to study various properties associated with protein-ligand interactions such as binding energy, hydrogen bonding, hydrophobicity and polarizability of donor and acceptor interaction (Shafiq et al., 2012).

Here, we describe the *in vitro* cytotoxic activity of the MeOH (90%) fraction of the methyl alcohol extract of the endophyte *Phialophora verrucosa* isolated from *Senecio flavus* (Asteraceae) leaves, as well as the isolation and identification of the metabolites and investigation of the potential molecular mechanism by docking simulation.

2. Experimental

2.1. General experimental procedures

ESI-MS spectral analysis performed on LC-MS HP1100 Agilent Finnigan LCQ Deca XP Thermoquest mass spectrometer. A Bruker DRX-400 spectrometer was used for measuring 1D and 2D NMR spectra (Bruker, USA). Chromatographic separations performed on silica gel 60 (0.04-0.063 mm, Merck, Germany). HPLC analysis performed on a Shimadzu LC-10ATVP apparatus equipped with a Shimadzu SPD-10A VP UV detector and Purospher® STAR RP-18e column (250 x 10 mm, 5 µm). TLC analysis achieved on pre-coated TLC plates with silica gel 60 F254 (0.2 mm, Merck, Germany).

2.2. Plant material

Senecio flavus Decne. Sch.Bip. (Asteraceae) collected in April 2015 from the plant wildly growing at the campus of Al-Azhar University, Assiut and authenticated by Prof. Dr. A.A. Fayed, Professor of Plant Taxonomy, Faculty of Science, Assiut University, Assiut, Egypt. A specimen has been deposited at the Department of Pharmacognosy herbarium, Al-Azhar University (SF.4.15).

2.3. Fungal material isolation and identification

The endophytic fungus *Phialophora verrucosa* Medlar. was isolated from the sterilized surface of a healthy leaf *Senecio flavus*. The leaf was first washed with distilled water, then immersed in 70% aqueous ethanol for 1 min, and rinsed in sterile distilled water. Finally, it was sliced into 2 × 2 cm pieces, with 3-4 pieces deposited on a petri dish containing potato dextrose agar plates (PDA, Difco), having gentamicin sulfate (200 mg/L) as an antibacterial agent, and plates were incubated at room temperature. Several fungi were found to grow exclusively out of the leaf tissue. From the growing fungi, a pure *Phialophora verrucosa* fungus was isolated by repeated re-inoculation on PDA plates (Elkhayat and Goda, 2017).

2.4. Identification of fungal strain

The fungus identified by Ph.D. Mohamad Taha, Department of Microbiology, Al-Azhar University, Assiut, Egypt, according to the characteristics of culture morphology and spore features (Campel et al., 2011). The fungus identified and a specimen has deposited at the Department of Pharmacognosy fungal herbarium, Al-Azhar University with the culture code (Phia.4.2015).

2.5. Cultivation of fungal strain

Mass cultivation of *P. verrucosa* was carried out in 8 Erlenmeyer flasks (1 L) for isolation and identification of the fungal metabolites. The fungus was grown on autoclaved rice solid medium (100 mL of distilled water added to 100 g commercially available rice) at room temperature under static conditions for 4 weeks (Elkhayat and Goda, 2017).

2.6. Isolation of secondary metabolites

The culture of *P. verrucosa* extracted with ethyl acetate (2 × 500 mL), and concentrated under vacuum to give 1.24 g of extract, which was partitioned between petroleum ether and 90% methanol in water. The hydromethanol fraction (0.93 g) subjected to vacuum liquid chromatography on silica gel eluted with gradient CH_2Cl_2: MeOH to give eight fractions (FI-FVIII). F-III (19 mg, CH_2Cl_2: MeOH 7:3) was chromatographed over silica gel eluted with petroleum ether: EtOAc (8:2, v/v) to afford compound 3 (2.8 mg). Purification of F-IV (16mg, CH_2Cl_2: MeOH 6:4) on semi-preparative HPLC using MeOH/H2O (7:3, *v/v*) afforded compounds 1 (3.2 mg) and 2 (3.7 mg) and F-V (21mg, CH_2Cl_2: MeOH 1:1) purified by semi-preparative HPLC using MeOH/H2O (75:25, *v/v*) afforded compounds 4 (4.2 mg) and 5 (2.9 mg). Other fractions were retained for further investigation.

2.7. Cytotoxic activity

The cytotoxic activity of the hydromethanolic fraction was tested against hepatic (HepG2) and breast (MCF-7) cancer cell lines by MTT assay as being previously reported by Barakat et al. (2019). Cell lines were obtained from VACSERA, Cairo, Egypt. Five serial dilutions of the tested sample and 5- fluorouracil were investigated, each experiment was done in triplicate, results were expressed as mean ± standard deviation and IC_{50} was calculated by Sigmaplot 12 software program.

2.8. Molecular simulation study

Molecular Operating Environment MOE program 2008.10 used for the molecular simulation (docking) study. Crystal structures of the vascular endothelial growth factor receptor (VGEFR-2) complexed with sorafenib (PDB ID: 4ASD), and of CDK-2 (PDB ID: 2DUV), CDK-4 (PDB ID: 1GIH) and of CDK-6 (PDB ID: 1XO2), were downloaded from the protein data bank. The downloaded crystal structures were prepared for docking by adding the missing protons, deleting water molecules and all unnecessary co-crystallized

ligands and metals using MOE software. Docking study performed using the software default parameters, and results of binding affinity to the active site were expressed as an energy score of binding (kcal/mol) (AbdElhameid et al., 2018).

3. Results and Discussion

3.1. Cytotoxic activity

The MTT assay was conducted to evaluate the anti-proliferative activity of the hydromethanolic fraction of the ethyl acetate extract of *P. verrucosa* against the breast cancer (MCF-7) and liver carcinoma (HepG-2) cell lines. Investigation of serial dilution of the fraction (100, 25, 6.25, 1.56 and 0.39 µg) revealed cell growth inhibition in a dose dependent manner for both cell lines (Table 1 and Fig. 1). According to the American National Cancer Institute guidelines, the extract having cytotoxic activity with an IC_{50} value < 30 µg/mL was considered as a promising platform for developing anticancer drugs (Mrid et al., 2019). The hydromethanolic fraction showed activity with an IC_{50} of 20.01 and 28.44 µg/mL, respectively, in comparison to 5-fluorouracil IC50 (11.05 and 12.46 µg/mL, respectively) (Fig. 2). Therefore, we applied the molecular docking to investigate the isolated polyketides to explore the active compound/compounds and the underlying mechanism.

Table 1
Cytotoxic activity of the MeOH (90%) fraction of the MeOH extract of *P. verrucosa*.

Conc µg/mL	100 µg	25 µg	6.25 µg	1.56 µg	0.39 µg
Phia/HepG2	37.99 ± 0.83	48.45 ± 1.37	59.08 ± 0.86	68.21 ± 0.37	79.53 ± 1.39
5FU/HepG2	33.61 ± 1.08	43.19 ± 1.19	53.48 ± 1.08	65.81 ± 2.08	76.28 ± 1.00
Phia/MCF7	39.43 ± 0.84	51.85 ± 1.20	61.27 ± 1.24	73.97 ± 1.64	80.39 ± 0.67
5FU/MCF7	35.15 ± 1.12	42.11 ± 0.70	55.8 ± 1.21	66.3 ± 1.11	78.27 ± 0.96

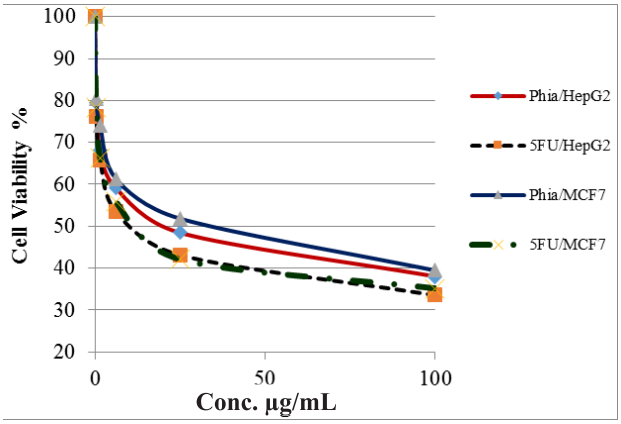

Fig. 1. Cytotoxic activity dose response curve of the MeOH (90%) fraction of *P. verrucosa.* extract.

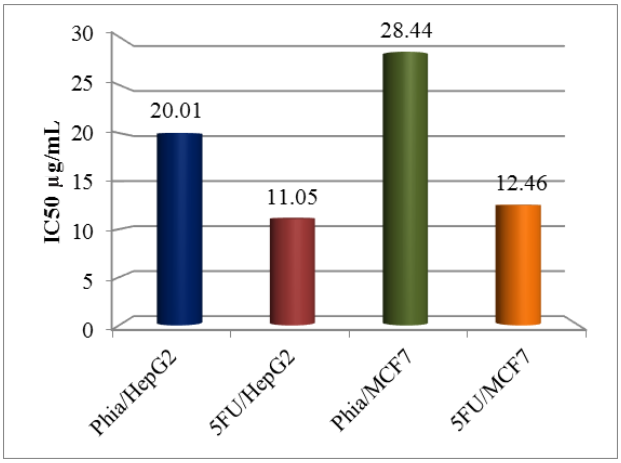

Fig. 2. IC_{50} of MeOH (90%) fraction of *P. verrucosa* alcoholic extract against HepG2 and MCF7 cell lines.

3.2. Compounds identification

The EI-MS spectrum of compound 1 (Fig. 3), obtained as a reddish-white needles, showed molecular ion peak at *m/z* 195 $[M+H]^+$. The ^1H and ^{13}C NMR (Table 2 and Table 3), spectra identified a tetralone structure, as the signals of two singlet aromatic methines at δH 6.13 (H-5) and 6.02 (H-8), an oxymethine at δH 4.17 (1H, m, H-3), two methylenes at δH 2.74 (2a) and 2.49 (2b), and at δH 2.71 (4a) and 2.98 (4b), in addition to a carbonyl signal at δC 202.3 (C-1). The COSY and HMBC experiments identified 1 as 3,6,7-trihydroxy-α-tetralone, previously isolated from *Phoma sp.* (Wang et al., 2012), and *Phialophora lagerbergii* (Alderidge et al., 1974), it is the first isolation of the compound from the *verrucosa* species.

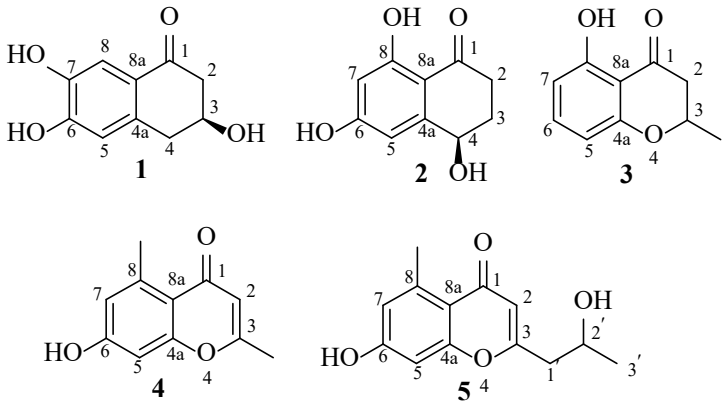

Fig. 3. Structures of isolated compounds **1-5** from *P. verrucosa*.

Compound 2 (Fig. 3), isolated as white needle crystals, with molecular ion peak at *m/z* 195 $[M+H]^+$, in the EI-MS spectrum. The ^1H and ^{13}C NMR (Table 2 and 3), were comparable to compound 1. The substitution pattern of the aromatic ring displayed two meta-coupled protons at δH 6.52 and 6.1 (*J* = 2.0 Hz), H-5 and H-7. The oxymethine at δH 4.65, two oxygenated aromatic methines at δC 162.3 and 166.3 (C-6 and C-8), identified compound 2 as 6-hydroxyisosclerone which was isolated from *Alternaria sp*. (Wang et al., 2017), and the deep sea fungus *Diaporthe phaseolorum* (Guo et al., 2019). This is the first isolation of 6-hydroxyisosclerone from the genus *Phialophora*.

Compound 3 (Fig. 3), isolated as a brownish residue, the EI-MS spectrum showed molecular ion peak at *m/z* 179 $[M+H]^+$. The ^1H and ^{13}C NMR spectra (Table 2 and 3), identified a benzopyrone nucleus as the set of proton signals owed to three aromatic methines at δH 6.41, 7.33 and 6.48 suggesting trisubstituted phenyl ring. The oxygenated methine at δC 73.8 (δH 4.56), aliphatic methylene 2.66 and 2.73, and a carbonyl at δC 198.5, in addition to the doublet methyl (1.51, 3H, d, *J* = 6.3 Hz) and the oxygenated aromatic carbon (δC 162.1) suggested a 5-hydroxy-2-methyl benzopyranone structure. Reviewing literatures confirmed 3 to be 2,3-dihydro-8-hydroxy-2-methyl-benzopyran-1-one isolated from *Phialophora gregata* (Gray et al., 1999) and *Hypoxylon haweianum* (Anderson et al., 1983), it is isolated from the *verrucosa* species for the first time.

Table 2

^1H (400 MHz), $CDCl_3$ of compounds **1-5**.

No.	Compounds δ_H (ppm, J in Hz)				
	1	2	3	4	5
2a	2.49 (1H, dd, J =17, 7.6 Hz)	2.48 (1H,m)	2.66 (1H, dd, J =17.2, 3.7 Hz)	6.02 (1H,s)	5.96 (1H, s)
2b	2.74 (1H, dd, J = 17, 4.0 Hz)	2.62 (1H,m)	2.73 (1H, dd, J = 17.2, 12.0 Hz)		
3	4.17 (1H, m)	1.9 (1H,m) 2.13 (1H,m)	4.56 (1H, m)	-	-
4a 4b	2.71 (1H,dd, J =16, 3.6 Hz) 2.98 (1H, dd, J =16, 3.2 Hz)	4.65 (1H,dd, 9.0, 4.0 Hz)	-	-	-
5 6	6.13 (1H, m) -	6.52 (1H,d, J = 2.0 Hz) -	6.41 (1H, dd, J = 8.3, 1.8 Hz) 7.33 (1H, dd, J = 8.3, 8.1 Hz)	6.65 (1H,d, J = 2.1 Hz) -	6.62 (1H, d, J = 1.8 Hz) -
7	-	6.10 (1H,d, J = 2.0 Hz)	6.48 (1H, J = 8.3, 1.8 Hz)	6.63 (1H, br.s)	6.58 (1H, d, J = 1.8 Hz)
8	6.02 (1H, s)	-	-	-	-
1′	-	-	-	-	2.56 (1H, m) 2.61 (1H, m)
2′	-	-	-	-	4.12 (1H, m)
3′	-	-	-	-	1.21 (3H, d, J = 6.1 Hz)
3-Me	-	-	1.51 (3H, d, J = 6.3 Hz)	2.33 (3H, s)	-
8-Me	-	-		2.64 (3H, s)	2.63 (3H, s)

Compound 4 (Fig. 3), obtained as a yellow viscous oil, EI-MS analysis showed pseudo-molecular ions at *m/z* 191.3 $[M+H]^+$ indicating a molecular weight of 190. The ^{1}H-NMR spectrum (Table 1) showed meta-coupled protons at δH 6.65 [d, *J* = 2.1 Hz] and 6.63 [brs], corresponding to H-7 and H-5, respectively. The vinylic singlet hydrogen H-2 at δH 6.02 and two singlet methyls at δH 2.33 and 2.64 ppm (CH_3-3 and CH_3-8, respectively). The COSY and HMBC experiments identified 3,8-dimethyl-7-hydroxychromone (Ayer and Racok, 1990; Orfali et al., 2017), known as altechromone A and previously isolated from *Alternaria sp*. (Orfali et al., 2017). This is the first isolation of altechromone A from the genus *Phialophora*.

Compound **5** (Fig. 3) isolated as a white amorphous powder. The NMR spectra were comparable to compound 4, with increment of 44 mass unit as the EI-MS exhibited a molecular ion at *m/z* 235.1 $[M + H]^+$. The ^{1}H and ^{13}C NMR spectral data (Table 2 and 3) revealed the presence of a terminal 2-hydroxy propyl residue as the doublet methyl at δH 1.21, oxymethine δH 4.12 and the methylene at δH 2.61. The H-H COSY and HMBC experiments assembled the 2′-hydroxy propyl residue at C-3 of 8-methyl-6-hydroxychromone nucleus, proofing compound 5 as 6-hydroxy-2-(2-hydroxypropyl)-8-methyl-4H-chromone, known as aloesol (Xu et al., 2009), previously isolated from the deep sea fungus *Diaporthe phaseolorum* (Guo et al., 2019), and from *Pestalotiopsis sp*. known as aloesol (Xu et al., 2009). It is isolated here for the first time from the genus *Phialophora*.

Table 3
^{13}C (100 MHz), $CDCl_3$ of compounds 1-5.

No.	Compounds δ_C (ppm)				
	1	**2**	**3**	**4**	**5**
1	202.3	203	198.5	170.3	177.8
2	47.4	36.1	43.8	110.7	110.2
3	66.9	33.1	73.8	163.2	167.8
4	39.2	68.1	-	-	-
4a	146	148.3	161.7	118.1	159.4
5	109	107.2	101.8	101.8	98.6
6	166.5	162.3	160.9	160.9	159.9
7	166.7	102.1	109.1	116.8	113.1
8	101.7	166.3	162.1	141.3	142.3
8a	117.1	109.7	108.3	159.2	114.7
1'	-	-	-	-	43.4
2'	-	-	-	-	65.8
3'	-	-	-	-	23.1
3-Me	-	-	20.8	19.7	-
8-Me	-	-	-	22.5	22.3

3.3. Molecular docking study of isolated compounds

Hepatocellular carcinoma (HCC) development involves different pathways and enzymes that promote cell division in unorganized ways. HCC is a highly vascularized tumor characterized by defects in the angiogenesis signalling pathway. Reduction of the pro-angiogenic enzymes as vascular endothelial growth factor receptor-2 (VEGFR-2), can reduce the angiogenesis and thus block the tumor growth. VEGF-2 is a growth factor that can be used as a target for HCC treatment (Meng, 2013; AbdElhameid et al., 2018). The cyclin-dependent kinases (CDKs) are also well-established targets for cancer treatment. They are key factors in cell cycle regulation and control of cell proliferation, especially CDK2, CDK4 and CDK6 (Hanse et al., 2009; Shi et al., 2015; Sherr et al., 2016). Thus, VEGFR-2 and CDKs inhibition is a promising and effective approach for new therapeutics of cancer treatment. Here, we utilized VEGFR-2 and CDKs as representative for angiogenesis and cell cycle regulation, respectively. The binding affinity score for the compounds are listed in Table 4. The docking score showed that compound **5** had the most stable binding energy to allosteric site of CDK-2 and 4. Meanwhile, compound **1** had the highest binding score to VEGFR-2 and CDK-6. In addition, compounds **2** and **3** displayed moderate affinity to examined proteins, while compound **4** was the least active.

Table 4
Docking score of the isolated compounds against different receptors.

Compound	VEGFR-2	CDK 2	CDK 4	CDK 6
1	-12.988	-11.872	-9.9778	-11.069
2	-9.8349	-8.9467	-8.0039	-9.1497
3	-9.8242	-8.859	-8.234	-8.7249
4	-9.2765	-7.1552	-7.9127	-8.3996
5	-12.668	-13.387	-12.269	-10.676

Fig. 4A shows that compound **5** interacts with CDK-2 receptor by forming weak hydrogen bond with the hydroxyl group of the side chain of Leu83 residues (bond lengths are 2.90 and 2.86 Å), while the Phe80 residue forms arene-arene interaction with the aromatic ring of **5**. In fact, the hydrophobicity plays an important role in the interaction of **5** with CDK-2 (Fig. 4A). In addition, compound **5** showed good affinity to CDK-4 (Fig.-4B) through hydrogen bonds between leu83 residues with the hydroxyl group of the side chain (bond distances are 2.46 and 2.53 Å). The involved hydrophobic interactions are Ile10, Val18, Ala31, Lys33, Phe80, Glu81, Phe82, Leu83, Leu134 and Asp145. Compound **1** showed high binding affinity to VEGFR-2 and CDK-6. It interacts with VEGFR-2 through formation of three hydrogen bonds with Glu885 (1.41 Å), Ile1025 (1.56 Å) and Asp1046 (1.33 Å) (Fig. 5A). It also interacts with CDK-6 through formation of three hydrogen bonds with Glu31 (1.58), Val150 (1.61)

and Leu 193 (1.42) (Fiq. 5B). The hydrophobic interactions involved in receptor binding (see Fig. 5).

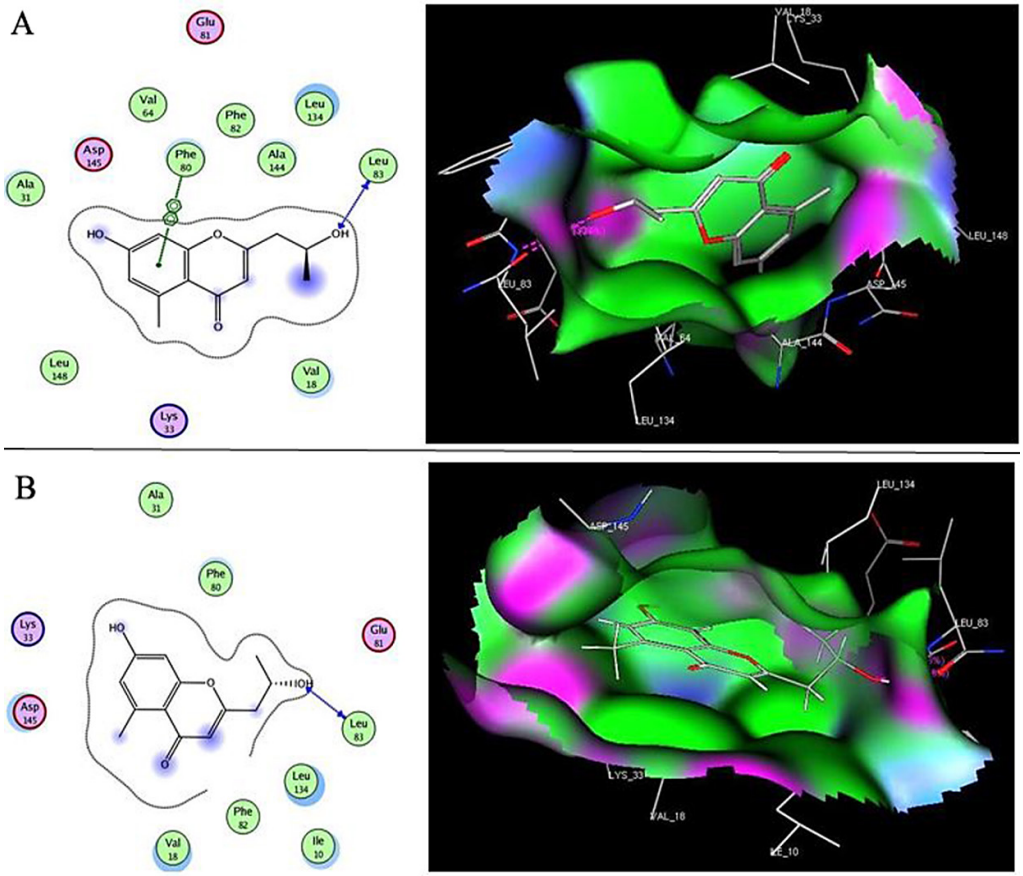

Fig. 4. 2D and 3D Ligand interactions of compound 5 with CDK-2 (A) and CDK-4 (B).

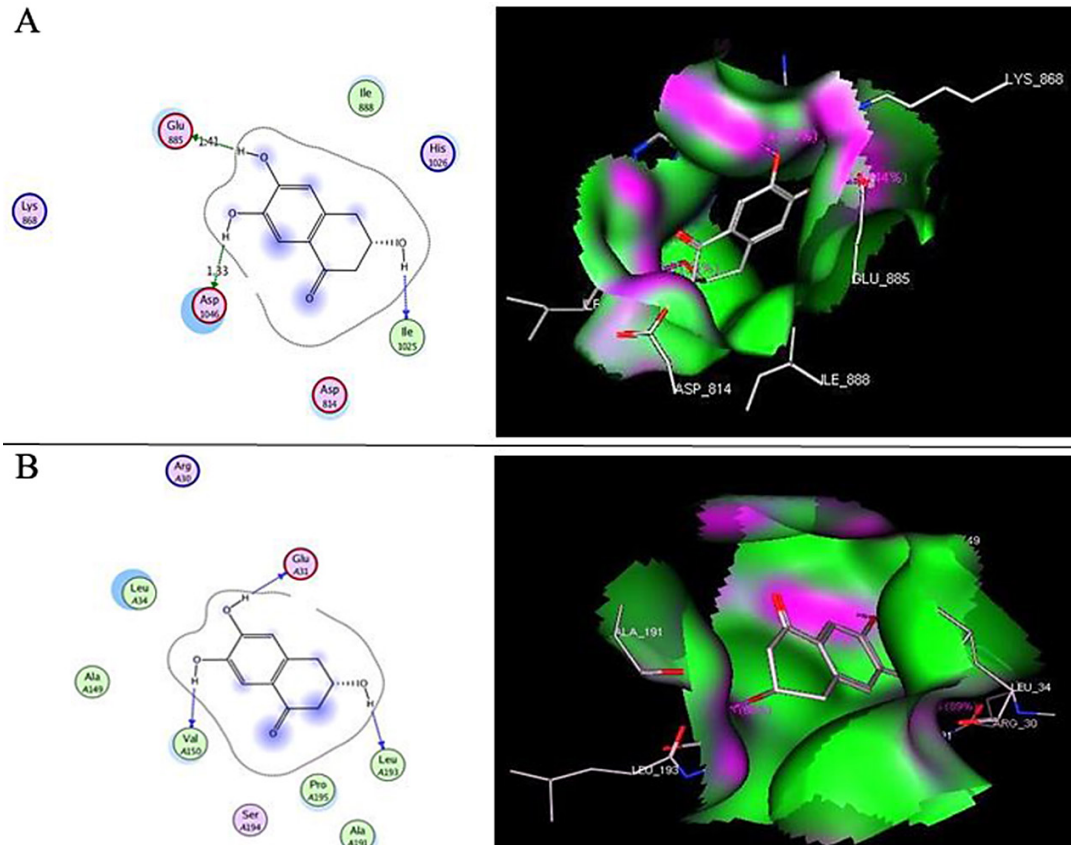

Fig. 5. 2D and 3D ligand interactions of compound **1** with VEGFR-2 (A) and CDK-6 (B).

4. Concluding remarks

P. verrucosa extract has shown cytotoxic activity against HepG2 and MCF-7 cell lines. Chromatographic isolation afforded five polyketides (1-5); of which compounds 2, 4 and 5 have been isolated for the first time from the genus *Phialophora*. Molecular docking study showed that compound 5 has the most stable binding energy to allosteric sites of CDK-2 and 4 with docking score -13.3865 and -12.269 kcal/mole respectively. While the highest binding score to VEGFR-2 and CDK-6 has associated with compound 1. Both compounds 1 and 5 are therefore promising candidates for anticancer molecules.

Acknowledgement

The authors are thankful to Prof. Dr. A. A. Fayed, Prof. of Plant Taxonomy, Faculty of Science, Assiut University, Egypt for plant identification, and for Dr. Mohamad Taha (Ph.D.), Department of Microbiology, Al-Azhar University, Assiut, Egypt for fungal identification.

Conflict of interest

The authors declare that there is no conflict of interest.

References

AbdElhameid, M.K., Labib, M.B., Negmeldin, A.T., Al-Shorbagy, M., Mohammed, M.R., 2018. Design, synthesis, and screening of *ortho*-amino thiophene carboxamide derivatives on hepatocellular carcinomaas VEGFR-2 inhibitors. J. Enzym. Inhib. Med. Chem. 33, 1472-1493.Alderidge, D.C., Davies, A.B., Jackson, M.R., Turner, W.B., 1974. Pentaketide metabolites of the fungus *Phialophora lagerbergii*. J. Chem. Soc. Perkin I, 1540-1541.

Anderson, J.R., Edwards, R.L., Whalley, A.J.S., 1983. Metabolites of the higher fungi. 3-Methyl-3,4-dihydroisocoumarins and related compounds from the ascomycete family xylariaceae. J. Chem. Soc. Perkin Trans 1, 2185-2192.

Arora, D., Sharma, C., Jaglan, S., Lichtfouse, E., 2019. Pharmaceuticals from Microbes: Impact on Drug Discovery. *in* Sharma N, Sharma V, Abrol V, Panghal A, Jaglan S. (Ed.). An Update on Bioactive Natural Products from Endophytic Fungi of Medicinal Plants. Springer International Publishing, Cham, pp. 122-153.

Ayer, W.A., Racok, J.S., 1990. The metabolites of *Talaromyces flavus*: Part 1. Metabolites of the organic extracts. Can. J. Chem. 68, 2085-2094.

Barakat, A., El-Senduny, F.F., Almarhoon, Z., Al-Rasheed, H.H., Badria, F.A., Al-Majid, A.M., Ghabbour, H.A., El-Faham, A., 2019. Synthesis, X-ray crystal structures, and preliminary antiproliferative activities of new s-triazine-hydroxybenzylidene hydrazone derivatives. J. Chem. https://doi.org/10.1155/2019/9403908.

Campbell, C.K., Johnson, E., Warnock, D.W., 2011. Identification of Pathogenic Fungi (2nd Ed.). Chichester: Wiley. ISBN 978-1444330700.

Chowdhury, N.S., Sohrab, M.H., Rana, M.S., Hasan, C.M., Jamshidi, S., Rahman, K.M., 2017. Cytotoxic naphthoquinone and azaanthraquinone derivatives from an endophytic *Fusarium solani*. J. Nat. Prod. 80, 1173-1177.

Elkhayat, E.S., Goda, A.M., 2017. Antifungal and cytotoxic constituents from the endophytic fungus *Penicillium* sp. Bull. Fac. Pharm. Cairo Univ. 55, 85-89.

El-Khayat, E.S., Ibrahim, S.R., Mohamed, G.A., 2012. Plant endophytes, renewable source of new natural products. Nat. Prod. J. 2, 225-234.

Gray, L.E., Gardner, H.W., Weisleder, D., Leib, M., 1999. Production and toxicity of 2,3-dihydro-5-hydroxy-2-methyl-4H-1-benzopyran-4-one by *Phialophora gregata*. Phytochemistry 50, 1337-1340.

Guo, H., Liu, Z.M., Chen, Y.C., Tan, H.B., Li, S.N., Li, H.H., Gao, X.X., Liu, H.Z., Zhang, W.M. , 2019. Chromone-derived polyketides from the deep-sea fungus *Diaporthe phaseolorum* FS431. Mar. Drugs 17, 182-193.

Hanse, E.A., Nelsen, C.J., Goggin, M.M., Anttila, C.K., Mullany, L.K., Berthet, C., Kaldis, P., Crary, G.S., Kuriyama, R., Albrecht, J.H., 2009. Cdk2 plays a critical role in hepatocyte cell cycle progression and survival in the setting of cyclin D1 expression *in vivo*. Cell Cycle 8, 2802-2809.

He, J-W, Wang, C-X, Yang, L, Chen, G-D, Hu, D, Guo, L-D, Yao, X-S, Gao, H., 2016. A pair of new polyketide enantiomers from three endolichenic fungal strains *Nigrospora sphaerica*, *Alternaria alternata*, and *Phialophora* sp. Nat. Prod. Commun. 11, 829-831.

Meng, X-Y, Zhang, H-X, Mezei, M., Cui, M., 2011. Molecular docking a powerful approach for structure-based drug discovery. Curr. Comput. Aided Drug Des. 7, 146-157.

Meng, F., 2013. Molecular dynamics simulation of VEGFR2 with sorafenib and other urea-substituted aryloxy compounds. J. Theor. Chem. http://dx.doi.org/10.1155/2013/739574

Mrid, B.R., Bouchmaa, N., Bouargalne, Y., Ramdan, B., Karrouchi, K., Kabach, I., El Karbane, M., Idir, A., Zyad, A., Nhiri, M., 2019. Phytochemical characterization, antioxidant and *in vitro* cytotoxic activity evaluation of *Juniperus oxycedrus* Subsp. *oxycedrus* Needles and Berries. Molecules 24, 502-520.

Nalli, Y., Mirza, D.N., Wani, Z.A., Wadhwa, B., Mallik, F.A., Raina, C., Riyaz-Ul-Hassan, S., Ali, A., 2015. Phialomustin A-D, new antimicrobial and cytotoxic metabolites from an endophytic fungus, *Phialophora mustea*. RSC Adv. 5, 95307-95312.

Orfali, R.S., Ebrahim, W., El-Shafae, A.M., 2017. Secondary metabolites from *Alternaria* sp., a fungal endophyte isolated from the seeds of *Ziziphus jujuba*. Chem. Nat. Compd. 53, 1031-1034.Rocha-Santos, T., Duarte, A.C., 2014. Introduction to the Analysis of Bioactive Compounds in Marine Samples. Comprehensive Analytical Chemistry 65, pp. 1-13.Shafiq, M.I., Steinbrecher, T., Schmid, R., 2012. Fascaplysin as a specific inhibitor for CDK4: insights from molecular modelling. PLoS One 7, e42612.

Sherr, C.J., Beach, D., Shapiro, G.I., 2016. Targeting CDK4 and CDK6: from discovery to therapy. Cancer Discov. 6, 353-367.

Shi, X-N., Li, H., Yao, H., Liu, X., Li, L., Leung, K-S., Kung, H-f., Lu, D., Wong, M-H., Lin, M.C., 2015. *In silico* identification and *in vitro* and *in vivo* validation of anti-psychotic drug fluspirilene as a potential CDK2 inhibitor and a candidate anti-cancer drug. PloS One 10, e0132072.

Strobel, G., Daisy, B., 2003. Bioprospecting for microbial endophytes and their natural products. Microbiol. Mol. Biol. Rev. 67, 491-502.

Wang, L., Xu, B., Wang, J., Su, Z., Lin, F., Zhang, C., Kubicek, C.P., 2012. Bioactive metabolites from *Phoma* species, an endophytic fungus from the Chinese medicinal plant *Arisaema erubescens*. Appl. Microbiol. Biotechnol. 93,1231-1239.

Weissman, K.J., Leadlay, P.F., 2005. Combinatorial biosynthesis of reduced polyketides. Nat. Rev. Microbiol. 3, 925-936.

Xu, J., Kjer, J., Sendker, J., Wray, V., Guan, H., Edrada, R., Lin, W., Wu, J., Proksch, P., 2009. Chromones from the endophytic fungus *Pestalotiopsis* sp. isolated from the Chinese Mangrove plant *Rhizophora mucronata*. J. Nat. Prod. 72, 662-665.

Ye, F., Chen, G-D., He, J-W., Li, X-X., Sun, X., Guo, L-D., Li, Y., Gao, H., 2013. Xinshengin, the first altenusin with tetracyclic skeleton core from *Phialophora* spp. Tetrahedron Lett. 54, 4551-4554.

Zhao, J., Wang, X., Sun, W., Mou, Y., Peng, Y., Zhou, L., 2013. Medium optimization for palmarumycin C13 production in liquid culture of endophytic fungus *Berkleasmium* sp. Dzf12 using response surface methodology. Electron. J. Biotechnol. 16, 16-26.